# Adsorption of Pulmonary Surfactant Protein SP-A to Monolayers of Phospholipids Containing Hydrophobic Surfactant Protein SP-B or SP-C: Potential Differential Role for Tertiary Interaction of Lipids, Hydrophobic Proteins, and SP-A†

Svetla G. Taneva‡ and Kevin M. W. Keough*,‡,§

*Department of Biochemistry and Discipline of Pediatrics, Memorial University of Newfoundland, St. John's, Newfoundland A1B 3X9, Canada*

*Received September 3, 1999; Revised Manuscript Received January 6, 2000*

ABSTRACT: Surface balance techniques were used to study the interactions of surfactant protein SP-A with monolayers of surfactant components preformed at the air−water interface. SP-A adsorption into the monolayers was followed by monitoring the increase in the surface pressure $\Delta\pi$ after injection of SP-A beneath the films. Monolayers of dipalmitoylphosphatidylcholine (DPPC):egg phosphatidylglycerol (PG) (8:2, mol/mol) spread at initial surface pressure $\pi_i = 5$ mN/m did not promote the adsorption of SP-A at a subphase concentration of 0.68 $\mu$g/mL as compared to its adsorption to the monolayer-free surface. Surfactant proteins, SP-B or SP-C, when present in the films of DPPC:PG spread at $\pi_i = 5$ mN/m, enhanced the incorporation of SP-A in the monolayers to a similar extent; the $\Delta\pi$ values being dependent on the levels of SP-B or SP-C, 3−17 wt %, in the lipid films. Calcium in the subphase did not affect the intrinsic surface activity of SP-A but reduced the $\Delta\pi$ values produced by the adsorption of the protein to all the preformed films independently of their compositions and charges. The divalent ions likely modified the interaction of SP-A with the monolayers through their effects on the conformation, self-association, and charge state of SP-A. Values of $\Delta\pi$ produced by adsorption of SP-A to the films of DPPC:PG with or without SP-B or SP-C were a function of the initial surface pressure of the films, $\pi_i$. In the range of pressures $5 \leq \pi_i \leq 35$ mN/m, where the monolayers existed in the liquid expanded (LE)/liquid condensed (LC) coexistence region, both the composition and the proportion of the LC phase in the films controlled the magnitude of $\Delta\pi$. Monolayers of DPPC:PG plus 17 wt % SP-B or SP-C, which had similar phase properties with LC phase occupying a maximum 25% of the total monolayer area, displayed different abilities to enhance the adsorption of SP-A to the surface. Results revealed that SP-B and SP-C in their pure monolayers had similar abilities in promoting the adsorption of SP-A, whereas SP-B, when present into the lipid films in the LE/LC coexistence state, displayed a higher capacity than SP-C to attract SP-A from the subphase. Lipid-induced changes in the conformations of the proteins might have modulated the interactions of SP-A with SP-B and SP-C incorporated into the phospholipid monolayers.

Pulmonary surfactant is a surface-active material composed of phospholipids (about 90%) and proteins (5−10%) that covers the alveolar epithelium. An interfacial layer enriched in DPPC[1] is likely responsible for the surface tension-reducing properties of lung surfactant. PG and surfactant-associated proteins are also required for the formation and the proper dynamics of the surfactant surface film in the airways. SP-A is the major pulmonary surfactant associated protein by mass (*1*). It is a hydrophillic glycoprotein with a monomeric molecular mass of 28−36 kDa and isoelectric points ranging from 4.8 to 5.2 (*2*). SP-A is characterized by a collagen-like N-terminal domain and variable glycosylation of the C-terminal region (*3*). The latter has binding sites for carbohydrates and calcium (*4*, *5*). Subunits of SP-A form trimers that associate into an octadecamer with a molecular mass of about 700 kDa (*6*). Porcine SP-B is a homodimer of disulfide-linked 79-residue monomers ($M_r = 18$ kDa) that contains regions of amphipathic α-helix and has a net charge of +12 (*7*). Porcine SP-C is a 35-amino acid residue protein that contains two thioester-linked palmitoyl groups giving a total molecular mass of 4.2 kDa. It has a 23-residue C-terminal α-helical portion and also has a net charge of +3 associated with residues near its N-terminal region (*8*). SP-B and SP-C are hydrophobic proteins soluble in organic solvents.

SP-A and SP-B have a cooperative calcium-dependent action in promoting surface activity of phospholipid mixtures

† This work was supported by the Medical Research Council of Canada.

* To whom correspondence should be addressed. Telephone: (709) 737-2530; fax: (709) 737-2552; e-mail: kkeough@morgan.ucs.mun.ca.

‡ Department of Biochemistry.

§ Discipline of Pediatrics.

[1] Abbreviations: DPPC, 1,2-dipalmitoyl-*sn*-glycero-3-phosphocholine; PG, L-α-phosphatidylglycerol (egg sodium salt); NBD-PC, 1-palmitoyl-2-[12-[(7-nitro-2-1,3-benzoxadiazol-4-yl)amino]dodecanoyl]-*sn*-glycero-3-phosphocholine; HEPES, *N*-(2-hydroxyethyl)piperazine-N′-(2-ethanesulfonic acid); EDTA, ethylenediaminetetraacetic acid; SP-A, surfactant protein A; SP-B, surfactant protein B; SP-C, surfactant protein C; Tris-HCl, tris(hydroxymethyl)aminomethane hydrochloride.

10.1021/bi992074x CCC: $19.00 
Published on Web 04/27/2000

(*9*) as well as in improving the resistance to inhibition by blood and plasma proteins (*10*). Synergy between SP-A and SP-B observed in the process of phospholipid membrane fusion in the presence of calcium has been attributed to specific calcium-dependent SP-A/SP-B interactions (*11*, *12*). Morphological studies have shown that in vitro reconstitution of SP-A with phospholipid bilayers containing SP-B in the presence of calcium produces a lattice-like array of bilayer structures similar to that of the native tubular myelin (*13*, *14*). SP-A promoted neither adsorption (*9*), fusion (*11*), or resistance to inhibition (*10*) of phospholipid liposomes containing SP-C, nor did it assemble tubular myelin in these lipid−protein combinations (*14*).

Tubular myelin is a unique three-dimensional structure that is a morphological form of pulmonary surfactant within the alveolar hypophase (*15*). Immunogold labeling of SP-A in tubular myelin has suggested that SP-A is located in the corners of this lattice-like structure (*16*). It has been proposed that SP-A binds lipid, SP-B, or both in the lattice corners, whereas self-association of SP-A oligomers stabilizes the structure (*4*). The function of this structure is unknown; however, it is widely considered to be the main source of the surface layer located at the alveolar interface. The above studies have suggested a role of SP-A/SP-B interactions in the biophysical and morphological properties of pulmonary surfactant phospholipids. However, it is uncertain whether the cooperativity between SP-A and SP-B in phospholipid reorganization is a result of specific binary protein−protein interactions or originates from more complex ternary lipid−protein−protein effects on phospholipid properties.

This paper reports on aspects of the specificity of the insertion of SP-A from the aqueous subphase into monolayers of SP-B or SP-C spread at the air−water interface. The influence of the lipid environment, in terms of surface pressure and phase properties, on the interactions of SP-A with SP-B or SP-C incorporated into lipid films was also studied by monitoring the adsorption of SP-A to spread monolayers containing DPPC:PG (8:2, mol/mol) plus SP-B or SP-C. The effects of calcium ions in the subphase on the association of SP-A with the spread monolayers of phospholipids and each hydrophobic protein were examined.

This study, which includes mixtures of phospholipid and proteins with particular ratios relevant to those used for reconstitution of tubular myelin in vitro, aids understanding of the molecular basis of the interactions among the pulmonary surfactant components.

## EXPERIMENTAL PROCEDURES

*Materials.* DPPC, Tris-HCl, EDTA, gramicidin D (from *Bacillus brevis*), melittin (from bee venom), and cytochrome *c* (from horse heart) were purchased from Sigma Chemical Co. (St. Louis, MO). NBD-PC and PG were obtained from Avanti Polar Lipids Inc. (Alabaster, AL), and sodium chloride and calcium chloride, reagent grade, were obtained from Fisher Scientific Co. (Ottawa, ON). DPPC and PG showed single bands on thin-layer chromatography on silica gel with a solvent system of chloroform−methanol−water (65:25:4 by vol) and were used without further purification.

*Protein Isolation.* Pig lungs were lavaged with 0.15 M NaCl, and the lavage was centrifuged at 800*g* for 10 min. The supernatant was centrifuged at 7000*g* for 60 min. The pellet was used for isolation of either SP-A or SP-B and SP-C. SP-A was purified from the surfactant pellet by extraction with 1-butanol (*4*, *17*). SDS−polyacrylamide gel electrophoresis (12% gel) was performed on samples of SP-A solutions (*18*) followed by staining with Coomassie Blue. Under reducing conditions (5% $\beta$-mercaptoethanol in the sample buffer), a major band at approximately 36 kDa and a minor band at about 28 kDa were observed.

SP-B and SP-C were prepared from the surfactant pellet independently of the SP-A preparation using chloroform−methanol as described previously (*7*, *19*). SP-B and SP-C were separated from the surfactant lipids and from each other by gel exclusion chromatography on Sephadex LH-60 (2.5 × 90 cm) using chloroform:methanol (1:1, v/v) acidified with 2 vol % of 0.1 N HCl. On SDS−polyacrylamide gel electrophoresis (16% gels) under nonreducing conditions, SP-B showed a major band at about 18 kDa and a minor one at about 29 kDa, whereas SP-C showed a single band at about 5 kDa. SP-B and SP-C were stored in chloroform:methanol (1:1, v/v). The data reported here represent results obtained with a single preparation each of SP-B or SP-C, whereas two different preparations of SP-A were used. Epifluorescence microscopy measurements with other preparations of SP-B and SP-C produced qualitatively similar images.

*Analytical Methods.* Concentrations of SP-A, SP-B, and SP-C were estimated by the fluorescamine method (*20*) using bovine serum albumin as a standard. The concentration of SP-A was also determined from the absorbance of its solutions at 277 nm and using the weight extinction coefficient for canine SP-A determined by King and MacBeth (*21*). Quantitative amino acid analysis (*22*) was used to verify the concentrations of SP-B and SP-C since the fluorescamine assay sometimes overestimated the concentrations of SP-C. Concentrations of DPPC, PG, and NBD-PC, dissolved in chloroform, were determined by measuring the phospholipid phosphorus (*23*, *24*). Water used in all experiments and analytical procedures was deionized and doubly distilled in glass, the second distillation being from dilute potassium permanganate solution.

*Surface Pressure−Time Measurements.* Adsorption measurements were performed at constant surface area in a Teflon dish ($R = 1.2$ cm) with a subphase volume of 5 mL of 145 mM NaCl, 5 mM Tris-HCl, and 2 mM EDTA, pH 6.9. Monolayers of DPPC:PG plus SP-B or SP-C were preformed at the air−water interface from chloroform−methanol solutions to give selected surface pressures, $\pi_i$. Monolayers of the water-soluble proteins, cytochrome *c*, melittin, and SP-A were preformed at $\pi_i$ by spreading from their aqueous solutions containing 0.1% amyl alcohol (*25*), whereas methanol was used to preform monolayers of gramicidin. The monolayer area was kept constant, and the surface pressure was raised by adding material dropwise. Fifteen minutes after monolayer spreading, desired volumes of SP-A in 5 mM HEPES were injected below the monolayer-covered surface through an injection septum. Surface tension was measured as a function of time by the Wilhelmy plate method, using a roughened platinum plate (perimeter of 2 cm) and a computer-controlled transducer readout, TSAR 1 (Tech-Ser Inc., Torrance, CA), connected to a chart recorder (Servoscribe). The subphase was stirred continuously with a Teflon-coated stirring bar and a magnetic stirrer at 22−24

°C. The effect of 5 mM $CaCl_2$ in the subphase buffer on the adsorption of SP-A in the presence or absence of preformed monolayers was examined.

*Epifluorescence Microscopy.* Epifluorescence microscopy and surface pressure−area measurements were performed on a surface balance whose construction and operation have been described previously (*26*, *27*). The trough design, however, had been modified, and it employed a continuous Teflon ribbon-barrier that prevented leakage of monolayer material. The lipids, DPPC, PG, and SP-B or SP-C were mixed in chloroform−methanol solutions, and 1 mol % NBD-PC (based on the lipid content) was added. NBD-PC partitions preferentially into the fluid (LE) phase of phospholipid monolayers. Monolayers were formed by spreading of the mixtures of DPPC:PG (8:2, mol/mol) containing 17 wt % SP-B or SP-C on subphases of 145 mM NaCl, 5 mM Tris-HCl, and 5 mM $CaCl_2$ (pH 6.9). After the mixtures were spread, 30 min was allowed for equilibration of the monolayers initially spread at about 0 mN/m. Films were compressed in 30 steps at a rate of 0.09 $nm^2$ $molecule^{-1}$ $min^{-1}$, and isotherms of surface pressure ($\pi$) versus monolayer area ($A_{mean}$) were recorded. At selected surface pressures, monolayers were observed through a 40× objective lens, and images were videorecorded. Each experiment, performed at 22−24 °C, took about 3 h. Usually 10 images at each surface pressure were analyzed using JAVA video analysis software (Jandel Scientific, Corte Madera, CA). The relative amounts of dark probe-excluding phase (percent dark phase) were determined and plotted as a function of the surface pressure (*27*).

Mean areas in the lipid−protein monolayers, $A_{mean}$, were calculated on the basis of molecules of lipid and numbers of amino acid residues of protein initially spread in the mixed films. Concentrations of SP-B or SP-C in the spread lipid−protein monolayers were defined as weight percent of protein or "residue" fraction, $X_r$, of the protein amino acid residues in the preformed protein−lipid monolayers calculated on the basis of molecules of lipids and numbers of amino acid residues of protein (*28*).

## RESULTS

*Adsorption of SP-A to Preformed Phospholipid Monolayers Containing SP-B or SP-C in the Absence of Calcium Ions in the Subphase.* Surface pressure $\pi$, defined as $\pi = \sigma_o - \sigma$, where $\sigma_o$ is the surface tension of the clean air−water interface and $\sigma$ is the surface tension of the protein solution, was measured as a function of time for various concentrations, $C_s$, of SP-A in the absence of preformed lipid−protein films. Constant surface pressures were reached in 120 min, and these values were plotted as a function of $C_s$ in Figure 1. Solutions of SP-A at a concentration of $C_s = 0.26$ $\mu$g/mL showed marginally detectable changes in $\pi$ ($\pi = 0.5$ mN/m at 120 min), and they did not induce significant surface pressure increases in monolayers of DPPC:PG (8:2, mol/mol) plus either SP-B or SP-C when $\pi_i = 5$ mN/m (data not shown). Monolayers of DPPC:PG containing SP-B or SP-C spread at $\pi_i = 5$ mN/m enhanced the attraction of SP-A to the surface from its solutions at $C_s = 0.68$ $\mu$g/mL as compared to the clean air−water interface (Figure 2), and this concentration of SP-A was chosen to study the interactions of the protein in the subphase with the spread lipid−protein films.

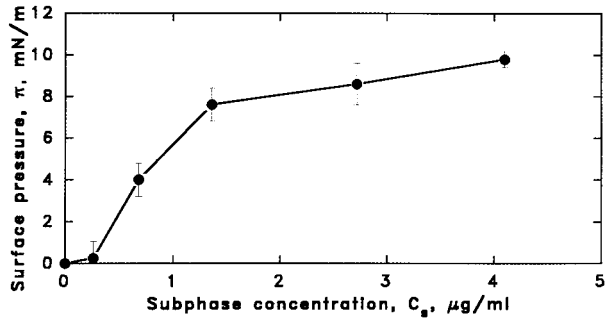


FIGURE 1: Surface pressure as a function of subphase concentration for adsorption of porcine SP-A from subphases containing 145 mM NaCl, 5 mM Tris-HCl, and 2 mM EDTA (pH 6.9) to monolayer-free surfaces. Error bars show the values for SD for two or three separate measurements. Adsorption time was 120 min.

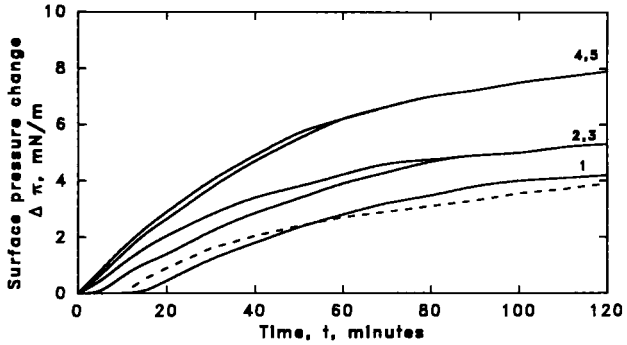


FIGURE 2: Curves of surface pressure increase after injection of SP-A (subphase concentration, 0.68 $\mu$g/mL) underneath monolayers of DPPC:PG (1), DPPC:PG plus 3 wt % SP-B (2), DPPC:PG plus 3 wt % SP-C (3), DPPC:PG plus 17 wt % SP-B (4), and DPPC:PG plus 17 wt % SP-C (5) preformed at an initial pressure 5 ± 1 mN/m. The dashed line represents the $\pi(t)$ curve for adsorption of SP-A to the monolayer-free interface. The subphase was 145 mM NaCl, 5 mM Tris-HCl, and 2 mM EDTA, pH 6.9. Duplicates for each monolayer were run, and the range of values for the average curves did not exceed 1 mN/m.

Monolayers of DPPC:PG, with or without SP-B or SP-C, were preformed at the air−water interface at $\pi_i = 5$ mN/m; after the injection of SP-A below the surface, $\pi$ was measured as a function of time. The change in surface pressure, $\Delta\pi = \pi - \pi_i$, defined as an increase in surface pressure induced by incorporation of SP-A into the preformed films, was plotted as a function of time. SP-A by itself displayed a measurable surface activity at $C_s = 0.68$ $\mu$g/mL (final surface pressure, 4 ± 0.5 mN/m, Figure 1); therefore, only $\Delta\pi > 4$ mN/m signifies an augmented attraction of SP-A to the interface caused by the preformed monolayers. At $\pi_i = 5$ mN/m, all of the preformed films studied were in similar fluid states; therefore, effects of different phase states of the preformed monolayers on the incorporation of SP-A into the films were avoided. Figure 2 shows the time dependence of the change in surface pressure $\Delta\pi$ following the injection of SP-A beneath the monolayers of DPPC:PG containing different concentrations of SP-B or SP-C. For comparison, the $\pi(t)$ curve for adsorption of SP-A to the clean air−water interface was plotted (dashed curve in Figure 2). Results indicated that films of DPPC:PG did not significantly promote the adsorption of SP-A as compared to its adsorption to the monolayer-free surface (compare curve 1 with the dashed curve in Figure 2). SP-B or SP-C at similar concentrations in the phospholipid monolayers enhanced the ability of SP-A to insert into the films to

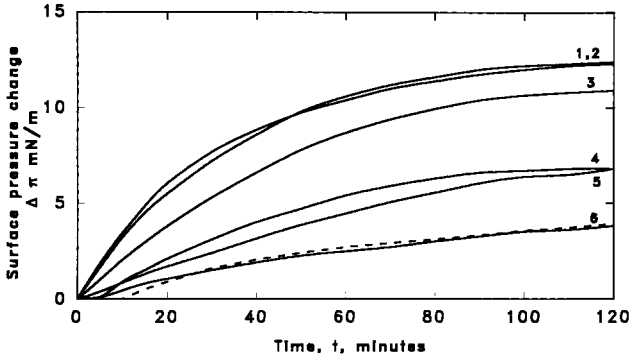


FIGURE 3: Surface pressure increase after injection of SP-A beneath monolayers of SP-B (1), SP-C (2), melittin (3), cytochrome *c* (4), gramicidin (5), and SP-A (6) spread at $\pi_i = 5$ mN/m. Concentration of SP-A was 0.68 $\mu$g/mL in 145 mM NaCl, 5 mM Tris-HCl, and 2 mM EDTA, pH 6.9. The dashed line represents the $\pi(t)$ profile for adsorption of SP-A to a monolayer-free interface. Duplicates were run, and the range of values for the average curves did not exceed 1 mN/m.

comparable extents, and the values for $\Delta\pi$ produced by adsorption of SP-A to the lipid−protein films increased with increasing levels of SP-B or SP-C in the monolayers (Figure 2). Note that the preformed lipid−protein monolayers contained similar levels of SP-B and SP-C when their concentrations were calculated as wt % protein or "residue" fraction of protein amino acid residues. However, approximately 4 times more molecules of SP-C than SP-B were present in the lipid−protein films.

The ability of SP-B and SP-C to promote insertion of SP-A into the preformed monolayers of DPPC:PG implied that protein−protein interactions might be involved in the attraction of the water-soluble protein SP-A to the film-covered surface. To investigate this possibility, monolayers composed only of single proteins of various charges and hydrophobicities were preformed at the air−water interface at $\pi_i = 5$ mN/m, and the change in $\Delta\pi$ during adsorption of SP-A to these films was monitored (Figure 3). Values of $\Delta\pi$ produced by adsorption of SP-A to the monolayers of either SP-B or SP-C were identical to each other (curves 1 and 2 in Figure 3) and similar to those measured for the adsorption of SP-A to preformed films of melittin (curve 3 in Figure 3). Porcine SP-B (dimer) and SP-C are positively charged proteins with a net charge of +12 and +3, respectively; their charges per amino acid residue are 0.075 and 0.085, respectively. They are hydrophobic proteins with polar/apolar ratios of approximately 0.22 and 0.11, respectively, calculated from their primary structures (*7*, *8*). Melittin is a basic polypeptide containing 5 positively charged amino acids per total of 26 residues, with a ratio of polar to apolar amino acid residues of 0.4 (*29*). Adsorption of SP-A to preformed monolayers of the hydrophillic basic cytochrome *c* [polar/apolar ratio of 2.04; p$I$ = 10.6 (*30*)] (curve 4, Figure 3) produced values of $\Delta\pi$ similar to those measured for the neutral, hydrophobic gramicidin D, which does not have polar amino acids (curve 5, Figure 3). Spread monolayers of SP-A did not enhance the adsorption of SP-A over that to the monolayer-free surface (curve 6, Figure 3).

*Effect of Calcium Ions on Interactions of SP-A in the Subphase with Preformed Monolayers at the Air−Water Interface.* Figure 4 demonstrates the effects of calcium ions at different concentrations in the subphase on the adsorption

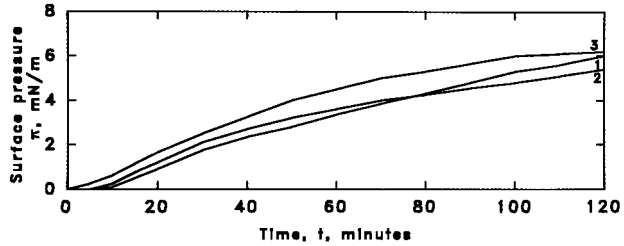


FIGURE 4: Effect of calcium ions on the adsorption of SP-A ($C_s$ = 1.36 $\mu$g/mL) to the monolayer-free interface from a subphase of 145 mM NaCl and 5 mM Tris-HCl, pH 6.9, containing 2 mM EDTA (1), 1.6 mM $CaCl_2$ (2), or 5 mM $CaCl_2$ (3).

of SP-A to the monolayer-free surface from solutions containing 145 mM NaCl and 5 mM Tris-HCl, pH 6.9 ($C_s$ = 1.36 $\mu$g/mL). Similar final surface pressures were measured for adsorption of SP-A in the presence or absence of 5 (curves 1 and 3) or 1.6 mM $CaCl_2$ (curve 2). Under these experimental conditions (high ionic strength buffers), calcium did not affect the surface activity of SP-A. Calcium-independent equilibrium values of surface pressure have also been reported for adsorption of dog SP-A from solutions of physiological salt concentrations (*31*).

SP-A exists in its native octadecameric form in buffers of low ionic strength at physiological pH (*6*). Calcium ions and high salt concentrations induce self-aggregation of SP-A (*5*, *32*); therefore, self-aggregation of SP-A possibly occurred under the experimental conditions used in these measurements. A threshhold concentration of 0.5 mM $Ca^{2+}$ has been reported to induce self-association of porcine SP-A, whereas at 1.6 mM $Ca^{2+}$, a level of calcium ions reported for the alveolar subphase of adult rabbit lungs (*33*), SP-A was only partially aggregated; the process of self-aggregation of SP-A was completed at about 5 mM $Ca^{2+}$ (*32*). In the following experiments, we used 5 mM $CaCl_2$ to evaluate effects of calcium-induced self-aggregation on the ability of SP-A to adsorb to preformed monolayers containing surfactant proteins and phospholipids. At $\pi_i = 5$ mN/m in the presence of calcium in the subphase, DPPC:PG monolayers that contained 17 wt % of either SP-B or SP-C marginally augmented the adsorption of SP-A to the surface, and final $\Delta\pi$ values comparable to those observed for adsorption of SP-A to the monolayer-free surface were measured (curves 1 and 2 in Figure 5). Although the divalent ions did not affect the intrinsic surface activity of SP-A (Figure 4), they attenuated the ability of the protein to interact with the lipid−protein monolayers preformed at the air−water interface (compare curves 1 and 2 in Figure 5 to curves 4 and 5 in Figures 2).

Addition of $Ca^{2+}$ to the subphase caused a similar reduction in $\Delta\pi$ produced by adsorption of SP-A to the single-component monolayers of SP-B and SP-C (compare curves 3 and 4 in Figure 5 to curves 1 and 2 in Figure 3) as well as those of melittin, cytochrome *c*, and gramicidin D (data not shown). Likewise, calcium ions suppressed the insertion of SP-A into monolayers of DPPC preformed at $\pi_i$ = 5 mN/m (data not shown). Thus, it appeared that calcium weakened the interactions of SP-A with the preformed monolayers regardless of their chemical compositions and charge states.

*Surface Pressure Dependence of $\Delta\pi$ Generated by the Adsorption of SP-A to Preformed Monolayers in the Presence of Calcium in the Subphase.* The adsorption of SP-A to

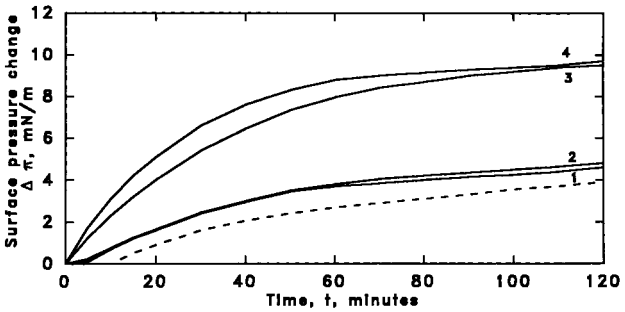


FIGURE 5: Surface pressure increase during adsorption of SP-A ($C_s = 0.68$ $\mu$g/mL) to monolayers of DPPC:PG plus 17 wt % SP-B (1), DPPC:PG plus 17 wt % SP-C (2), SP-B (3), and SP-C (4) in the presence of 5 mM $CaCl_2$ in a subphase of 145 mM NaCl and 5 mM Tris-HCl, pH 6.9. Films were spread at $\pi_i = 5$ mN/m. The dashed curve represents the $\pi(t)$ isotherm for SP-A to the monolayer-free surface. Duplicates were run for each monolayer, and the range of values for the average curves did not exceed 1 mN/m.

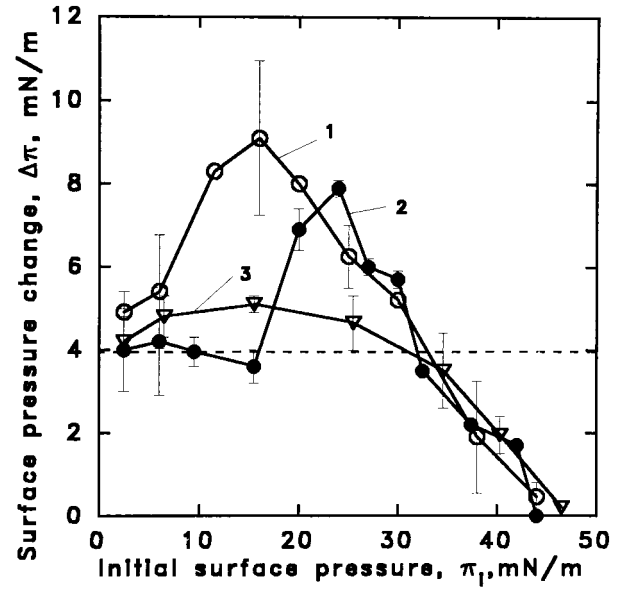


FIGURE 6: Effect of the initial surface pressure on surface pressure increase after injection of SP-A underneath monolayers of DPPC:PG (1), DPPC:PG plus 17 wt % SP-B (2), and DPPC:PG plus 17 wt % SP-C (3). Concentration of SP-A was 0.68 $\mu$g/mL in a subphase of 145 mM NaCl, 5 mM Tris-HCl, and 5 mM $CaCl_2$. Error bars show values of SD for two to four measurements for each surface pressure. The dashed line represents the value of surface pressure measured for adsorption of SP-A to the monolayer-free interface.

monolayers of DPPC:PG alone or supplemented with 17 wt % SP-B or SP-C was examined as a function of the initial surface pressure of the monolayers, $\pi_i$ (Figure 6). For each experiment, a new monolayer was spread at $\pi_i$, and the increase of surface pressure $\Delta\pi$ produced by adsorption of SP-A from the subphase was monitored as a function of time. Constant values for $\Delta\pi$ were attained within 120 min, and these values were plotted as a function of $\pi_i$ in Figure 6. Note that only values of $\Delta\pi > 4$ mN/m, which was the pressure attained during adsorption of SP-A from solutions at $C_s = 0.68$ $\mu$g/mL to the monolayer-free surface, signify augment of adsorption of SP-A by the preformed films. At $\pi_i \leq 5$ mN/m, the preformed monolayers existing in the LE phase did not enhance the insertion of SP-A into the surface over that seen for the clean surface, and similar $\Delta\pi$ values were measured for the three systems (Figure 6). At $\pi_i \geq 35$ mN/m, SP-A adsorbed to all preexisting monolayers; however, values of $\Delta\pi$ lower than those observed for the adsorption of SP-A to the monolayer-free surface were measured. At surface pressures $5 < \pi_i < 35$ mN/m, the three plots in Figure 6 showed dependencies on $\pi_i$ characteristic of each of the preformed monolayers. In this range of surface pressures, where the films existed in the LE (liquid expanded)/LC (liquid condensed) coexistence region, both the composition and the phase properties of the preformed films likely regulated the adsorption of SP-A to the surface. The plot of $\Delta\pi(\pi_i)$ for adsorption of SP-A to monolayers of DPPC:PG displayed maximal increase in surface pressure at $\pi_i \approx 15$ mN/m. Incorporation of SP-A into films of DPPC:PG supplemented with 17 wt % SP-B led to maximal $\Delta\pi$ values at $\pi_i \approx 23$ mN/m, whereas the adsorption of SP-A to films of DPPC:PG plus 17 wt % SP-C produced only marginal increases in the surface pressure in the range of surface pressures $5 \leq \pi_i \leq 30$ mN/m. The results indicated that SP-B and SP-C, which when reconstituted with DPPC:PG at $\pi_i = 5$ mN/m similarly promoted the insertion of SP-A into the monolayers (curves 1 and 2 in Figure 5), modified the adsorption of SP-A in different patterns as the initial surface pressure of the films increased.

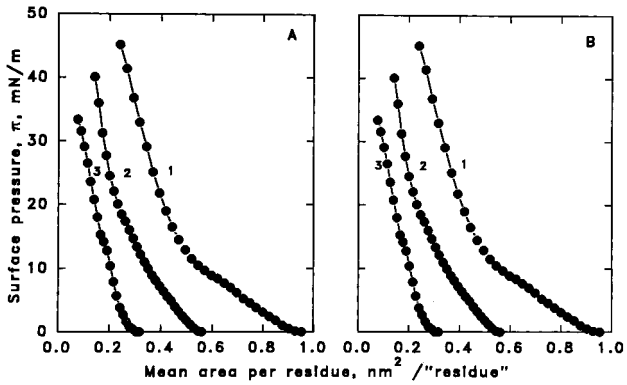


FIGURE 7: Isotherms of surface pressure versus mean area per "residue" for spread monolayers of (A) DPPC:PG (1), DPPC:PG plus 17 wt % SP-B or $X_r = 0.58$ (2), and SP-B (3); (B) DPPC:PG (1), DPPC:PG plus 17 wt % SP-C or $X_r = 0.56$ (2), and SP-C (3). "Residue" was defined as an amino acid or a phospholipid molecule. Each monolayer contained 1 mol % (based on phospholipid content) of NBD-PC. The subphase was 145 mM NaCl, 5 mM Tris-HCl, and 5 mM $CaCl_2$, pH 6.9.

*Epifluorescence Microscopy on Spread Monolayers of DPPC:PG Plus SP-B or SP-C in the Presence of Calcium in the Subphase.* Since surface pressure-induced lateral phase separation occurs in the systems studied, we examined the effects of their phase properties on the adsorption of SP-A. Figure 7A,B show the compressional isotherms for DPPC:PG alone or supplemented with 17 wt % SP-B or SP-C. Maximal equilibrium surface pressures of about 40−45 mN/m were reached during the stepwise compression of the films during the simultaneous surface pressure−area/epifluorescence microscopic measurements. However, dynamic surface pressure of 72 mN/m was reached in films of DPPC:PG during their continuous compression at 0.16 $nm^2$ $molecule^{-1}$ $min^{-1}$. The pressure−area curves for the single-component monolayers of either SP-B or SP-C were consistent with the isotherms already reported for these proteins (*19*).

Representative epifluorescence micrographs for monolayers of DPPC:PG (8:2, mol/mol) are shown in Figure 8.

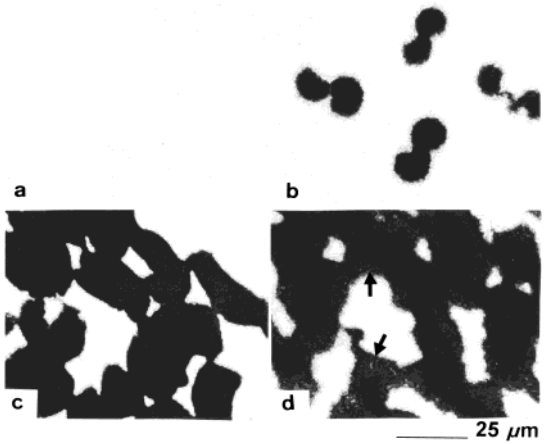


FIGURE 8: Epifluorescent images of monolayers of DPPC:PG (8:2, mol/mol) at selected surface pressures 5 (a), 10 (b), 25 (c), and 35 mN/m (d). The subphase was 145 mM NaCl, 5 mM Tris-HCl, and 5 mM $CaCl_2$, pH 6.9. Arrows point to a gray phase distinct from the black probe-excluding phase.

Microscopic observations of monolayers of single-component monolayers of DPPC have been already described in detail (*34*). Monolayers of PG existed in fluid or LE phase as indicated by the appearance of a single homogeneously fluorescent phase at all surface pressures up to 44 mN/m (images not shown). Monolayers of DPPC:PG showed pressure-induced lateral segregation of dark probe-excluding LC regions and bright probe-including regions of LE phase, similar to those observed in mixed films of saturated and unsaturated phospholipids (*34*). At $\pi \leq 5$ mN/m, the films existed in the homogeneous LE state (Figure 8a), whereas at higher pressures black domains, likely comprising phospholipid in LC phase, nucleated and grew in size with increasing surface pressure (Figure 8b−d). At surface pressures of about 30 mN/m, charcoal-gray phase (arrows in Figure 8d) surrounding the edges of the black domains appeared, and the probe-excluding condensed phases coexisted with the fluorescent LE phase up to the highest pressures measured (about 45 mN/m). Note that the video-recorded images are represented in black/gray/white, whereas the films were seen in black/gray/green when observed via the eyepiece of the microscope. A possible explanation for the different intensities of darkness of the condensed phases is that, unlike the black probe-excluding condensed phase formed at the low surface pressures, the charcoal-gray condensed phase formed at the high surface pressures included some of the fluorescent dye that aggregated and self-quenched when it was forced to be in the condensed phase (*35*). Alternatively, the biphasic appearance of the probe-excluding phases seen in the micrographs at $\pi > 30$ mN/m could be interpreted as follows: The black phase was formed by nearly pure DPPC, and the gray phase likely contained some amounts of PG and hence had a packing density and dye solubility different from those of the DPPC-enriched black probe-excluding phase.

Typical images seen in monolayers of DPPC:PG plus 17 wt % SP-B or SP-C are shown in Figure 9A,B. At low surface pressures of about 2 mN/m, the visual fields were heterogeneous, showing lateral probe distribution: dark probe-excluding domains of nearly circular shapes (drop-like, doughnut-like, or ring-like) in a bright green fluorescent background (Panels a in Figure 9A,B). These domains did not change in shape or size as the surface pressure increased to 5 mN/m. As surface pressure was further increased (7−8 mN/m), new probe-excluding dark domains of irregular shapes, likely comprising phospholipids in LC state, appeared and grew larger with increasing surface pressure (small arrows in Panels b in Figure 9A,B). At $\pi \approx 10$ mN/m, their size was commensurate with that of the dark circular domains (big arrows in Panels b in Figure 9A,B) that had appeared at the low pressure. On further compression, at $\pi \approx 15-17$ mN/m, the dark condensed domains became corrugated, whereas a few unchanged circular domains were still observed at these pressures. At $\pi \geq 17-20$ mN/m, the latter were no longer detected in the visual fields, and the dark probe-excluding LC domains coexisted with the bright probe-including LE phase that persisted up to the highest surface pressures measured in these experiments (approximately 40 mN/m) (Panels c in Figure 9A,B).

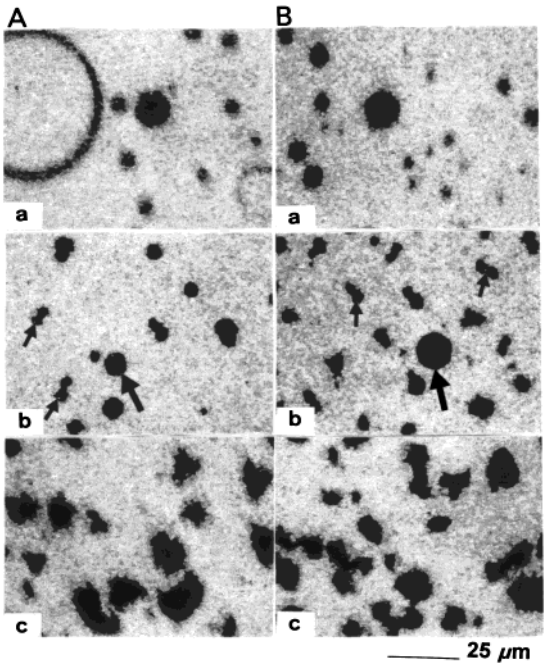


FIGURE 9: Epifluorescent images of monolayers of DPPC:PG plus 17 wt % SP-B (A) or SP-C (B) at selected surface pressures of 2 (a), 10 (b), and 25 mN/m (c). The subphase was 145 mM NaCl, 5 mM Tris-HCl, and 5 mM $CaCl_2$, pH 6.9. Small and large arrows represent two putatively different fractions of probe-excluding phases (see text for discussion about them).

The presence of probe-excluding regions in the lipid−protein films at low surface pressures (Panels a in Figure 9A,B) where the monolayers of DPPC:PG exist in the homogeneous LE state (Figure 8a) suggested that these domains, which occupied about 5% of the total area at $\pi =$ 5 mN/m, were likely protein-induced, and possibly protein-enriched, phases. Similar dark circular domains occupied about 1% of the total monolayer area at $\pi = 5$ mN/m in monolayers of DPPC:PG (8:2, mol/mol) that contained 3 wt % of either SP-B or SP-C (data not shown). Probe-excluding domains of circular shapes were also seen at low surface pressures in monolayers of the individual phospholipids, DPPC or PG, supplemented with 17 wt % SP-B or SP-C (data not shown). These findings were consistent with a protein-induced phase separation in the monolayers independently of the presence of the LE−LC transition in the monolayers of the lipids alone. Thus, an influence of the

phospholipid LE−LC phase transition and phospholipid condensed phase on the formation of the probe-excluding phase at the low surface pressures was ruled out. Observations on films of PG with 17 wt % SP-B or SP-C, which do not exhibit a LE−LC phase transition (and therefore LC probe-excluding phase did not appear with increasing surface pressure), showed that at $\pi \approx 20-25$ mN/m the dark circular domains disappeared, and a homogeneous LE lipid−protein phase was formed. As discussed, circular probe-excluding domains were discerned up to surface pressures of about 17−20 mN/m in the films of DPPC:PG plus 17 wt % SP-C or SP-B.

The exact origin or molecular structure of these probe-excluding domains that are apparently not condensed-phase lipids is uncertain. Although surface pressures of 20−25 mN/m seem to be too high for the existence of a gaseous phase, it could be that the probe-excluding circular domains represented a gaseous phase that was originally trapped at low surface pressures (about 0 mN/m) within the LE phase. With increasing surface pressure, the contents of the gaseous phase were dispersed into the fluid phase. Experimental evidence supporting this hypothesis was obtained by expansion and recompression of films of SP-B/PG (17 wt % SP-B) initially compressed to surface pressures above the characteristic pressure where the circular probe-excluding domains disappeared and homogeneously fluorescent LE phase was formed ($\pi > 25$ mN/m). On film expansion, the probe-excluding domains did not appear, and the monolayers remained homogeneously fluorescent up to very low surface pressures, $\pi \leq 0.2$ mN/m. During further expansion in the low-pressure region, circular probe-excluding phase appeared and grew in size with increasing the film surface. This phase, likely in a gaseous state, was incorporated into the films during their recompression and was seen in the monolayers up to 25 mN/m where the recompressed films acquired an homogeneous appearance. A similar evolution of the circular probe-excluding domains with expansion and recompression was seen in the films of DPPC:PG plus 17 wt % SP-B, although in the presence of the probe-excluding LC phase in these films, it was more difficult to distinguish between the shapes of the probe-excluding domains. These experiments suggested that SP-B and SP-C evoked changes in the phospholipid physical state so that the gaseous phase formed at very low (not detectable) surface pressures endured compression to high surface molecular densities and coexisted with the traditional phospholipid LE and LC phases up to relatively high surface pressures (about 20−25 mN/m). The fact that during expansion of the compressed films the gaseous phase did not reappear in stages exactly reverse to those during compression suggested that it was not in equilibrium with the coexisting LE and LC phases. It is noteworthy that relatively high compressional speeds were employed in this study, and more thorough experiments will be necessary to determine the equilibrium properties of the circular probe-excluding domains.

To determine whether an alternative interpretation that the latter were protein-separated phases was feasible, monolayers of DPPC:PG (8:2, mol/mol) containing 17 wt % of SP-B or SP-C labeled with fluorescein, and not containing NBD-PC, were observed through the fluorescence of the protein fluorophores. Nonfluorescent circular domains, similar to those seen in the films of SP-B/(DPPC:PG) and SP-C/(DPPC:PG) visualized via the fluorescence of NBD-PC, were detected at low surface pressures ($\pi \approx 5$ mN/m), and occasional dot-like phases of very bright fluorescence, probably consisting of aggregates of pure SP-B or SP-C, were also seen (data not shown). These observations implied that the circular domains that were visualized as dark phases via the protein fluorophores were not aggregates of pure proteins. More likely they comprised lipid−protein gaseous phase that appeared dark due to quenching of both the lipid and the protein fluorophores by interactions with the water subphase. This speculation is based on previous studies on the liquid−gas transition in monolayers of stearic acid. The gaseous regions in these films appeared dark due to quenching of the NBD fluorophores when they were in contact with water in the gaseous state where the film density is relatively low and the molecules lie flat on the water surface (*36*). Spectra of fluorescein-labeled molecules have been reported to be sensitive to solvent polarity and pH (*37*).

Gray probe-excluding domains of circular shapes similar to those observed in the present study have been induced by adsorption of the amphiphilic peptide bombolitin III into films of DPPC at low surface pressures (*38*). These domains have been observed via the fluorescence of a lipid probe and, according to the author's interpretation, consisted of phase-separated peptide that contained some phospholipid doped with the fluorescent probe (*38*).

Epifluorescence microscopy of monolayers of phospholipids plus critical concentrations of cholesterol has indicated a coexistence of immiscible fluid phases that undergo reversible two-phase to one-phase transformation at a characteristic surface pressure (*39*−*41*). The biphasic appearance of the fluid−fluid coexistence region has been attributed to the exclusion of the fluorescent lipid probe from one of the fluid phases that was cholesterol-rich and had a structure more ordered than that of the traditional LE phase (*41*). We cannot entirely dismiss the possibility that the circular probe-excluding domains induced by SP-B and SP-C in the phospholipid films were a fluid phase of a particular order different from that of the traditional phospholipid LE phase. However, the continuum of the circular probe-excluding domains observed during compression/expansion/recompression of the monolayers between the gaseous and the LE states provides experimental support for their ascription to the gaseous phase.

*Quantitation of the Dark Domains.* The transition of a monolayer from LE to LC phase upon compression has been quantitatively described by parameters such as size and number of condensed domains and percentage of condensed phase as a function of the surface pressure (*27*, *42*). The relative area of dark probe-excluding domains (percent dark phase) was determined and plotted as a function of the surface pressure for monolayers of DPPC:PG (Figure 10A) and DPPC:PG plus 17 wt % SP-B or SP-C (Figure 11). The phase properties of the films, in terms of percent dark phase, were related to their abilities to promote the adsorption of SP-A to the surface. We note that in the adsorption experiments, in which the $\Delta\pi(\pi_i)$ dependencies were determined, the initial surface pressures $\pi_i$ were attained by adding sequential aliquots of the lipid−protein solutions to the surface at constant surface area, whereas the phase properties of the monolayers (percent dark phase) were assessed from epifluorescence microscopic observations at surface pressures

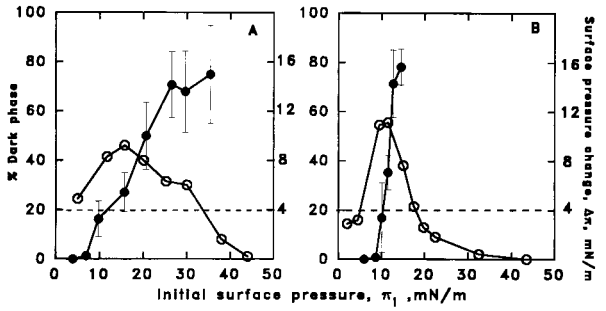


FIGURE 10: Percent dark (probe-excluding) area as a function of the surface pressure in monolayers of DPPC:PG (A) and DPPC (B) spread on 145 mM NaCl, 5 mM Tris-HCl, and 5 mM $CaCl_2$ (filled symbols). Error bars indicate mean ± SD for 10 images analyzed at each surface pressure. Hollow symbols represent the plots for surface pressure increase induced by adsorption of SP-A to films of DPPC:PG (A) and DPPC (B) preformed on the same subphase at initial surface pressure $\pi_i$. Dashed line represents the value of surface pressure measured for adsorption of SP-A to the monolayer-free surface.

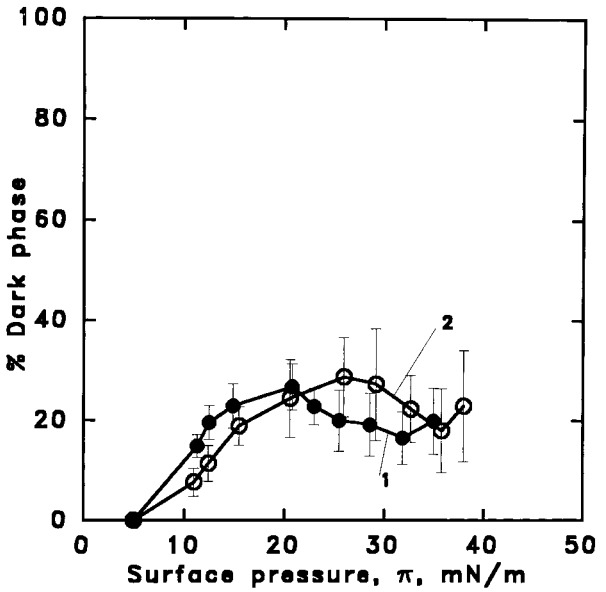


FIGURE 11: Percent dark (probe-excluding) phase as a function of the surface pressure for monolayers of DPPC:PG plus 17 wt % SP-B or $X_r = 0.58$ (1, ●) and DPPC:PG plus 17 wt % SP-C or $X_r = 0.56$ (2, ○). Error bars represent ± SD for 10 images analyzed at each surface pressure. The subphase was 145 mM NaCl, 5 mM Tris-HCl, and 5 mM $CaCl_2$.

that were attained by compression of the monolayers initially formed at $\pi \approx 0$ mN/m. Direct comparison of $\Delta\pi(\pi_i)$ plots with those of percent dark phase ($\pi$), therefore, is based on the assumption of physical equivalence of the monolayers formed by the two different methods. It has been shown that the surface pressure−area diagram for monolayers of DPPC obtained by dropwise application of material to the surface differs at the high surface pressures from that obtained by reduction of the surface area (*43*). Incomplete incorporation of material in the films formed by addition of material at constant surface area likely determined the differences observed (*43*).

The diagram $\Delta\pi(\pi_i)$ for the DPPC:PG monolayers (Figure 6) was replotted and compared with data for percent dark phase for the same system in Figure 10A. The appearance of the LC phase at $\pi > 5$ mN/m augmented the adsorption of SP-A to the DPPC:PG films, and $\Delta\pi$ increased proportionately to the relative amount of the LC phase in the range of surface pressures $5 \leq \pi \leq 15$ mN/m. A further increase in surface pressure, which led to an increase in percent dark phase, diminished the adsorption of SP-A, likely because of the higher lateral packing of the phospholipid monolayers at the high pressures. As noted earlier, only values of $\Delta\pi >$ 4 mN/m, a value measured for adsorption of SP-A to the clean air−water interface, signify enhanced adsorption of SP-A to the monolayer-covered as compared to the monolayer-free surface.

The phase transition from the LE to LC state in single-component monolayers of DPPC had a similar activation effect on the adsorption of SP-A to the preformed phospholipid films. Figure 10B compares the adsorption profile of SP-A to monolayers of DPPC, $\Delta\pi(\pi_i)$, with the plot of percent dark phase ($\pi$). The onset of the phase transition and the presence of coexisting phases augmented the adsorption of SP-A from the subphase to the spread monolayers of DPPC as compared to the surface pressure measured for adsorption of SP-A to the clean air−water interface (dashed line in Figure 10B).

The 17 wt % of either SP-B or SP-C in the films of DPPC:PG reduced the percent dark phase in the films to ∼25% at $\pi \approx 20-25$ mN/m, the two proteins having similar effects on a weight basis (Figure 11). This observation was consistent with the previously observed perturbation of packing and inhibition of condensed phase formation in phospholipid monolayers by the two proteins (*44*−*46*). The values of percent dark phase in Figure 11 were determined as area of dark probe-excluding regions without discrimination for different domain shapes. Therefore, at $\pi < 17-20$ mN/m, the values for percent dark phase included the areas of the circular probe-excluding, possibly gaseous, domains that were different from the conventional LC phase. As discussed already, the proportion of those domains was about 5% of the total monolayer area at $\pi = 5$ mN/m.

The data in Figure 11 indicate that, in terms of relative area of probe-excluding phase, SP-B and SP-C modified the phase properties of the phospholipid monolayers in similar patterns. Nevertheless, the effects of SP-B and SP-C on the adsorption of SP-A to the preformed films were quite different when each hydrophobic protein was incorporated into phospholipid films in the LE/LC coexistence state (Figure 6). It appeared that in the presence of calcium ions in the subphase, the preformed monolayers of DPPC:PG plus SP-C only marginally augmented the adsorption of SP-A at any of the initial surface pressures studied, even when there was up to 25% probe-excluding LC phase in the monolayers (Figures 6 and 11). In the presence of SP-B in the DPPC:PG monolayers, the adsorption of SP-A was elevated in a characteristic manner (Figures 6 and 11).

## DISCUSSION

Incubation of SP-A with bilayers of DPPC:PG containing SP-B, but not SP-C, in the presence of $Ca^{2+}$ produced a lattice-like structure very similar to that of the native tubular myelin (*13, 14*). Adsorption of SP-A to the lipid/hydrophobic protein bilayers likely represents a step in the process of reorganization of the lipid structure by SP-A. Adsorption of SP-A to "preformed" lipid−protein films may play an important role upon administration of therapeutic lipid

surfactant that contains SP-B and SP-C. In the present study, we have used monolayer models to examine the interactions of SP-A, adsorbing from the subphase, with preformed monolayers of DPPC:PG alone or supplemented with SP-B or SP-C. The property of SP-A to adsorb and produce additional increases in surface pressure in preexisting lipid and lipid−protein monolayers was studied in a broad range of surface pressures between 2.5 and 45 mN/m (Figure 6). This range of surface pressures includes the physiologically relevant surface tension of ∼30 mN/m measured at total lung capacity (*47*). It also includes surface pressures at which a correspondence between monolayer and bilayer lipid states has been proposed, from $\pi \approx 20$ (*48*) to 50 mN/m (*49*).

Measurements were performed at 22−24 °C with ambient water vapor pressure. Although the temperature in the lungs is much higher, it is still lower than the transition temperature from gel to liquid crystalline state for DPPC ($T_c = 41$ °C), which is the most considerable component of pulmonary surfactant. At 37 °C, DPPC still undergoes the LE to LC phase transition (*50*, *51*). DPPC:PG (8:2, mol/mol) is in the transition region between the gel and the liquid crystalline phase in the range between 23 and 38 °C (*52*), and differential scanning calorimetry of native rabbit surfactant, which contains all surfactant lipids and proteins, has shown a broad melting curve with an onset temperature of about 10 °C and a completion temperature of about 45 °C (*53*). Temperature and humidity did not affect the values of the equilibrium surface tension measured for adsorbed films from dog surfactant (*54*). These results implicate that while there may be some quantitative differences between measures of the interactions of SP-A with the lipid or lipid−protein films at 22−24 and 37 °C, the major qualitative factors defining their properties are likely to be the same at the two temperatures.

SP-A exhibited an intrinsic tendency to adsorb to the clean air−water interface from solutions containing physiological salt concentrations (Figure 1). In the absence of calcium in the subphase, monolayers of DPPC:PG alone preformed at surface pressures associated with the LE state ($\pi = 5$ mN/m) only marginally enhanced the adsorption of SP-A above that to the monolayer-free surface, whereas the addition of either SP-B or SP-C to the lipid films considerably augmented the adsorption of SP-A as compared to the clean air−water interface (Figure 2); maximal increase of surface pressure was measured for SP-A adsorbing to the monolayers of SP-B or SP-C alone (Figure 3). This result implied a potential role for protein−protein interactions in the process of insertion of SP-A into the lipid films containing hydrophobic surfactant protein. Adsorption of SP-A to monolayers of melittin, a basic protein with an estimated hydrophobicity not very different from those of SP-B and SP-C, produced $\Delta\pi$ values similar to those measured for SP-B and SP-C (Figure 3). This result implied that nonspecific interactions might have determined the association of SP-A with the pure protein monolayers of SP-B or SP-C.

Adding calcium ions to the subphase (145 mM NaCl; 5 mM Tris-HCl) did not affect the adsorption of SP-A to a clean interface (Figure 4), but it reduced the adsorption of SP-A to all monolayers studied (compare Figure 5 with Figures 2 and 3). Calcium ions induce self-association of the intact SP-A (*5*, *32*) and a conformational change in the C-terminal fragment of the protein (*5*). They may also reduce the charge density of SP-A, an acidic protein of p*I* in the range of 4.8−5.2 (*2*), and thus modify its polar interactions with the preformed monolayers. Therefore, the cations might have weakened the interactions of SP-A with the monolayers of the positively charged proteins, SP-B, SP-C, melittin, and cytochrome *c*, through neutralization of the anionic sites of SP-A. Since calcium ions also suppressed the adsorption of SP-A to the monolayers of the neutral gramicidin and the zwitterionic DPPC, it is possible that, through their effects on the conformation and aggregation of SP-A, the cations attenuated the hydrophobic component of interactions of the protein with the preformed monolayers.

The phase state of the preformed monolayers affected the adsorption of SP-A to the monolayer-covered interfaces. In the presence of calcium in the subphase, films of DPPC:PG plus SP-B or SP-C in the LE state ($\pi_i = 5$ mN/m) did not augment the adsorption of SP-A; the surface pressure change induced by the adsorption of SP-A to these films was comparable to the value measured for adsorption of SP-A to the monolayer-free surface. An increase in the surface pressure of the preformed monolayers, $\pi_i$, which was accompanied by a phase transition from the LE to the LC state, enhanced the adsorption of SP-A to the preformed films as compared to its adsorption to the clean surface in patterns characteristic of the different monolayers (Figure 6). Comparison of the plots of percent dark phase ($\pi$) in the monolayers and $\Delta\pi$ ($\pi_i$) produced by adsorption of SP-A to these films revealed that the appearance of LC phase augmented the adsorption of SP-A (Figure 10). This observation is consistent with a preferential accommodation of the $Ca^{2+}$-aggregated SP-A at the line boundary between the LE and the LC phases. Such a preferential binding of proteins to the coexistence region in phospholipid monolayers have been observed experimentally for SP-A (*55*) and discussed theoretically (*56*). A positive correlation between the percent dark (LC) phase in the preformed monolayers of DPPC and DPPC:PG and the change of surface pressure produced by adsorption of SP-A to these films was observed up to about 12−15 mN/m (Figure 10). At $\pi > 15$ mN/m, other factors, such as high lipid packing densities and larger areas occupied by LC films, likely hindered the penetration of SP-A in the preformed monolayers and hence reversely affected the values of $\Delta\pi$ produced by the adsorption of SP-A.

We observed an intriguing result that the ability of SP-B and SP-C to enhance the adsorption of SP-A to lipid−protein films varied with the lipid environment. The two proteins similarly augmented SP-A adsorption when they formed pure protein monolayers or when they were included into DPPC:PG films in the LE state (Figure 5). However, when present in the monolayers of DPPC:PG in the LE/LC coexistence region, SP-B and SP-C exhibited different abilities to enhance the adsorption of SP-A (Figure 6). The monolayers of SP-B/(DPPC:PG) and SP-C/(DPPC:PG) had similar phase properties in terms of percent dark phase (Figure 11) and number and size of LC domains (data not shown). Therefore, effects of different areas and peripheral perimeters of LC domains on the adsorption of SP-A into the two monolayer systems could be excluded. Likewise, different distributions of SP-B and SP-C in the lipid monolayer phases could not account for their abilities to interact differently with SP-A in the subphase, since epifluorescence microscopy has shown that fluorescently labeled SP-B and SP-C occupy the LE

phase of monolayers of DPPC (*46*) and DPPC:PG (unpublished observations). Therefore, differences in the abilities of the monolayers of SP-B/(DPPC:PG) and SP-C/(DPPC:PG) to incorporate SP-A could not be related to their mesoscopic properties.

On a molecular level, there are a few factors that should be considered when comparing the binary interactions of SP-A with SP-B or SP-C with the ternary SP-A/SP-B (or SP-C)/lipid interactions. Potential electrostatic interactions of the acidic SP-A with the basic SP-B or SP-C incorporated into the films of DPPC:PG could be affected by the net charge of the films containing the negatively charged PG. An estimation showed that SP-B and SP-C, which have similar net positive charge per amino acid residue, brought equal positive charge to the monolayers of DPPC:PG. Therefore, the ratios between the protein (SP-B or SP-C) positive and the PG negative charges were similar for the two protein−lipid monolayers.

Since differences were observed in the adsorption profiles of SP-A to SP-B or SP-C only when the latter were incorporated into the lipid monolayers in the LE/LC state (Figure 6), an assumption could be made that the binary SP-A/SP-B or SP-A/SP-C interactions were influenced by putative lipid-induced alterations in the protein conformations. SP-B and SP-C have been shown by circular dichroism (*57*) and external reflection absorption infrared spectroscopy (*58*) to have stable structures in lipid monolayers, whereas adsorption of SP-A to monolayers of DPPC caused the formation of extensive protein fibrous networks, a likely result of lipid-promoted SP-A−SP-A interactions (*59*). Binding of SP-A to lipid vesicles in the gel state caused conformational changes in the protein molecule that affected its intrinsic fluorescence (*60*) and its accessibility to trypsin degradation (*32*). A recent transmission electron microscopy study has also indicated that lipid-induced structural changes in SP-A occurred during binding of the protein to lipid bilayers (*61*). These findings, implying that the conformation of SP-A is more prone to lipid-induced modifications than those of SP-B and SP-C, allow speculations that the adsorption of SP-A to the lipid/protein monolayers was likely accompanied by lipid-induced conformational changes in SP-A that might have modulated its interactions with SP-B and SP-C incorporated into the films so that stronger attraction of SP-A to the lipid films plus SP-B than those plus SP-C occurred. A hypothesis that lipid-induced protein conformational changes trigger interactions of SP-A with SP-B but not with SP-C may accommodate the observations of cooperative effects between SP-A and SP-B but not SP-C on some properties of lipid systems (*9*−*12*). A model of lipid-induced $Ca^{2+}$-dependent conformational change in SP-A, which could trigger protein−protein interactions between the carbohydrate recognition domains of SP-A, has already been put forward to explain aggregation of phospholipid vesicles by SP-A (*32*).

The results from this study revealed a composite picture of interactions of SP-A in the subphase with phospholipid monolayers containing the hydrophobic protein SP-B or SP-C. These interactions were dependent on the extent of condensation and the lateral molecular packing of the preformed monolayers. The attenuation of SP-A adsorption by calcium ions possibly resulted from $Ca^{2+}$-induced structural changes in SP-A and was not simply a charge neutralization. In the monolayer model, $Ca^{2+}$ was not required for the intimate interactions of SP-A with a single lipid or lipid−protein monolayer, an observation that is consistent with findings of calcium-independent binding of SP-A to phospholipid bilayers (*60*−*62*). In other studies, the divalent cations were prerequisite for the SP-A-induced aggregation of phospholipid vesicles (*4*, *11*) and the formation of tubular myelin in vitro (*13*, *14*). In the latter studies, in addition to a potential role in altering the interactions of SP-A with phospholipid bilayers, the divalent ions were likely necessary to modify the charge and hydration states of apposed monolayers from adjacent bilayers, which were required to come in close proximity for the bilayer properties examined. Interestingly, SP-A did not dissociate from converted (collapsed) tubular myelin in response to calcium chelation (*63*), a finding supporting the idea that $Ca^{2+}$ is not required for the SP-A−lipid interactions during assembly of tubular myelin.

In conclusion, the monolayer measurements showed lack of specificity in the binary interactions of SP-A with SP-B or SP-C. Specificity in interactions of SP-A with SP-B was only seen when lipids were present, and SP-A could not be substituted for by concanavalin A in the specific ternary SP-A−SP-B−lipid interactions (unpublished observations). Specific ternary, or higher order, lipid−protein interactions in the presence of calcium ions may all participate in the assembly of tubular myelin in vivo. The relative importance of the various components in these interactions needs to be further elucidated.

## REFERENCES


1. King, R. J., and Clements, J. A. (1972) *Am. J. Physiol. 223*, 707−714.
2. Sueishi, K., and Benson, B. J. (1981) *Biochim. Biophys. Acta 665*, 442−453.
3. Hawgood, S., Efrati, H., Schilling, J., and Benson, B. J. (1985) *Biochem. Soc. Trans. 13*, 1092−1096.
4. Haagsman, H. P., Hawgood, S., Sargeant, T., Buckley, D., White, R. T., Drickamer, K., and Benson, B. J. (1987) *J. Biol. Chem. 262*, 13877−13880.
5. Haagsman, H. P., Sargeant, T., Hauschka, P. V., Benson, B. J., and Hawgood, S. (1990) *Biochemistry 29*, 8894−8900.
6. King, R. J., Simon, D., and Horowitz, P. M. (1989) *Biochim. Biophys. Acta 1001*, 294−301.
7. Curstedt, T., Johansson, J., Barros-Söderling, J., Robertson, B., Nilsson, G., Westberg, M., and Jörnvall, H. (1988) *Eur. J. Biochem. 172*, 521−525.
8. Curstedt, T., Johansson, J., Persson, P., Eklund, A., Robertson, B., Löwenadler, B., and Jörnvall, H. (1990) *Proc. Natl. Acad. Sci. U.S.A. 87*, 2985−2989.
9. Hawgood, S., Benson, B. J., Schilling, J., Damm, D., Clements, J. A., and Tyler White, R. (1987) *Proc. Natl. Acad. Sci. U.S.A. 84*, 66−70.
10. Venkitaraman, A. R., Hall, S. B., Whitsett, J. A., and Notter, R. H. (1990) *Chem. Phys. Lipids 56*, 185−194.
11. Poulain, F. R., Allen, L., Williams, M. C., Hamilton, R. L., and Hawgood, S. (1992) *Am. J. Physiol. 262*, L730-L739.
12. Poulain, F. R., Nir, S., and Hawgood, S. (1996) *Biochim. Biophys. Acta 1278*, 169−175.
13. Suzuki, Y., Fujita, Y., and Kogishi, K. (1989) *Am. Rev. Respir. Dis. 140*, 75−81.
14. Williams, M. C., Hawgood, S., and Hamilton, R. L. (1991) *Am. J. Respir. Cell Mol. Biol. 5*, 41−50.
15. Gil, J., and Reiss, O. K. (1973) *J. Cell Biol. 58*, 152−171.
16. Voorhout, W. F., Veenendaal, T., Haagsman, H. P., Verkleij, A. J., Van Golde, L. M. G., and Geuze, H. J. (1991) *J. Histochem. Cytochem. 39*, 1331−1336.

17. Taneva, S., McEachren, T., Stewart, J., and Keough, K. M. W. (1995) *Biochemistry 34*, 10279−10289.
18. Laemli, U. K. (1970) *Nature 227*, 680−685.
19. Taneva, S., and Keough, K. M. W. (1995) *Biochim. Biophys. Acta 1236*, 185−195.
20. Udenfriend, S., Stein, S., Bohlen, P., Dairman, W., Loimgrukes, W., and Weigele, M. (1972) *Science 178*, 871−872.
21. King, R. J., and MacBeth, M. C. (1979) *Biochim. Biophys. Acta 557*, 86−101.
22. Sarin, V. K., Gupta, S., Leung, T. K., Taylor, V. E., Ohning, B. L., Whitsett, J. A., and Fox, J. L. (1990) *Proc. Natl. Acad. Sci. U.S.A. 87*, 2633−2637.
23. Bartlett, G. R. (1959) *J. Biol. Chem. 234*, 466−468.
24. Keough, K. M. W., and Kariel, N. (1987) *Biochim. Biophys. Acta 902*, 11−18.
25. Birdi, K. S. (1989) *Lipid and Biopolymer Monolayers at Liquid Interfaces*, p 153, Plenum Press, New York.
26. Nag, K., Boland, C., Rich, N. H., and Keough, K. M. W. (1990) *Rev. Sci. Instrum. 61*, 3425−3430.
27. Nag, K., Rich, N. H., Boland, C., and Keough, K. M. W. (1991) *Biochim. Biophys. Acta 1068*, 157−160.
28. Taneva, S., and Keough, K. M. W. (1994) *Biochemistry 33*, 14660−14670.
29. *The Merck Index: An Encyclopedia of Chemicals, Drugs and Biologicals* (1983) p 829, Merck & Co., Inc., Rahway, NJ.
30. Mita, T. (1989) *Bull. Chem. Soc. Jpn. 62*, 2299−2306.
31. Efrati, H., Hawgood, S., Williams, M. C., Hong, K., and Benson, B. J. (1987) *Biochemistry 26*, 7986−7993.
32. Ruano, M. L. F., Miguel, E., Pérez-Gil, J., and Casals, C. (1996) *Biochem. J. 313*, 683−689.
33. Nielson, D. W. (1984) *Pediatr. Res. 17*, 386A.
34. Nag, K., and Keough, K. M. W. (1993) *Biophys. J. 65*, 1019−1026.
35. Klausner, R. D., and Wolf, D. E. (1980) *Biochemistry 19*, 6199−6203.
36. Moore, B., Knobler, C. M., Broseta, D., and Rondalez, F. (1986) *J. Chem. Soc., Faraday Trans. 82*, 1753−1761.
37. Haugland, R. P. (1996) *Handbook of Fluorescent Probes and Research Chemicals* (Spence, M. T. Z., Ed.) p 14, Molecular Probes, Inc., Eugene, OR.
38. Signor, G., Mammi, S., Peggion, E., Ringsdorf, H., and Wagenknecht, A. (1994) *Bichemistry 33*, 6659−6670.
39. Subramaniam, S., and McConnell, H. M. (1987) *J. Phys. Chem. 91*, 1715−1718.
40. Rice, P. A., and McConnell, H. M. (1989) *Proc. Natl. Acad. Sci. U.S.A. 86*, 6445−6448.
41. Worthman, L.-A., Nag, K., Davis, P. J., and Keough, K. M. W. (1997) *Biophys. J. 72*, 2569−2580.
42. Peschke, J., and Möhwald, H. (1987) *Colloids Surf. 27*, 305−323.
43. Lösche, H., and Möhwald, H. (1984) *Colloids Surf. 10*, 217−224.
44. Pérez-Gil, J., Nag, K., Taneva, S., and Keough, K. M. W. (1992) *Biophys. J. 63*, 197−204.
45. Nag, K., Pérez-Gil, J., Cruz, A., and Keough, K. M. W. (1996) *Biophys. J. 71*, 246−256.
46. Nag, K., Taneva, S., Pérez-Gil, J., Cruz, A., and Keough, K. M. W. (1997) *Biophys. J. 72*, 2638−2650.
47. Bachofen, H., Schürch, S., Urbinelli, M., and Weibel, E. R. (1987) *J. Appl. Physiol. 62*, 1878−1887.
48. Marcelja, S. (1974) *Biochim. Biophys. Acta 367*, 165−172.
49. Nagle, J. F. (1976) *J. Membr. Biol. 27*, 233−250.
50. Albrecht, O., Gruler, H., and Sackmann, E. (1978) *J. Phys. 39*, 301−313.
51. Crane, J. M., Putz, G., and Hall, S. B. (1999) *Biophys. J. 77*, 3134−3143.
52. De Fontanges, A., Bonté, F., Taupin, C., and Ober, R. (1984) *J. Colloid Interface Sci. 101*, 301−308.
53. Keough, K. M. W., Farrell, E., Cox, M., Harrell, G., and Taeusch, H. W., Jr. (1985) *Can. J. Physiol. Pharmacol. 63*, 1043−1051.
54. Wldeboer-Venema, F. (1980) *Respir. Physiol. 39*, 63−71.
55. Ruano, M. L. F., Nag, K., Worthman, L.-A., Casals, C., Pérez-Gil, J., and Keough, K. M. W. (1998) *Biophys. J. 74*, 1101−1109.
56. Netz, R. R., Andelman, D., and Orland H. (1996) *J. Phys. (Paris) 6*, 1023−1047.
57. Oosterlaken-Dijksterhuis, M. A., Haagsman, H. P., van Golde, L. M. G., and Demel, R. A. (1991) *Biochemistry 30*, 10965−10971.
58. Pastrana-Rios, B., Taneva, S., Keough, K. M. W., Mautone, A. J., and Mendelsohn, R. (1995) *Biophys. J. 69*, 2531−2540.
59. Palanyar, N., Ridsdale, R. A., Possmayer, F., and Harauz, G. (1998) *Biochem. Biophys. Res. Commun. 250*, 131−136.
60. Casals, C., Miguel, E., and Perez-Gil, J. (1993) *Biochem. J. 296*, 585−593.
61. Palaniyar, N., Ridsdale, R. A., Holterman, C. E., Inchley, K., Possmayer, F., and Harauz, H. (1998) *J. Struct. Biol. 122*, 297−310.
62. King, R. J., Carmichael, M. C., and Horowitz, P. M. (1983) *J. Biol. Chem. 258*, 10672−10680.
63. Williams, M. C. (1992) in *Pulmonary Surfactant from Molecular Biology to Clinical Practice* (Robertson, B., Van Golde, L. M. G., and Batenburg, J. J., Eds.) pp 87−107, Elsevier, Amsterdam, The Netherlands.

BI992074X